Fermi National Accelerator Laboratory

FERMILAB-Pub-87/226-T
ETH-PT/87-7
December, 1987

Photoproduction and electroproduction of heavy flavours with gluon bremsstrahlung

R. K. Ellis
Fermi National Accelerator Laboratory
P. O. Box 500, Batavia, Illinois 60510
Z. Kunszt*
Institute of Theoretical Physics,
ETH - Hönggerberg, Zürich, Switzerland
and
Fermi National Accelerator Laboratory
P. O. Box 500, Batavia, Illinois 60510

Abstract

We present compact expressions for the cross sections due to the subprocesses $\gamma + g \to Q + \bar{Q} + g$ and $\gamma + q \to Q + \bar{Q} + q$, including the dependence on the mass m of the heavy quark. These reactions give $O(\alpha_S)$ corrections to the $O(\alpha_S \alpha)$ subprocess $\gamma + g \to Q + \bar{Q}$ which describes the electro- and photoproduction of a heavy quark pair from a hadron target in the leading order of perturbation theory. Using these formulae we have calculated the cross section for the electroproduction of heavy quarks with hard gluon bremsstrahlung both at the energy of HERA and above. We have also estimated the contributions of the reactions $g + g \to Q + \bar{Q}$ and $q + \bar{q} \to Q + \bar{Q}$, which enter also at order $\alpha_S^2 \alpha$. Our results indicate that gluon bremsstrahlung is less important for electroproduction and photoproduction than for hadroproduction.

*On leave of absence from the Central Research Institute of Physics, Budapest

Operated by Universities Research Association Inc. under contract with the United States Department of Energy

I. INTRODUCTION

The study of charm[1] and bottom production[2,3] as well as the search[4] for the top quark are important goals at the present generation of hadron machines. This interest will certainly persist both at the Tevatron and $Sp\bar{p}S$ collider, as well as at the SSC and LHC. In this paper we investigate an alternative method of studying similar physics. We study the production of heavy flavours using either a photon beam, or a high energy electron beam such as is provided by HERA[5].

Theoretical arguments[6] indicate that the cross sections for heavy flavour production in hadron-hadron, photon-hadron and electron-hadron collisions can be reliably calculated in perturbative QCD. The short distance cross-sections are calculable as a perturbation series in the running coupling constant with corrections which are suppressed by powers of the heavy quark mass. However, the theoretical estimates, available in the literature, are at best semi-quantitative[7,8,9]. There are two major uncertainties. Firstly, the gluon wave function of the proton has not yet been extracted from the data with the desired accuracy. Secondly, the important next to the leading order contributions have not been included in the calculations. In the case of hadron-hadron collisions certain higher order effects have been discussed in terms of hard gluon bremsstrahlung cross sections with a cutoff on the transverse momentum of the final state gluon[7,9]. A complete higher order calculation for the hadroproduction of heavy flavours has recently been presented in ref. [10].

In the case of photoproduction and electroproduction even such a qualitative analysis has yet to be performed, since the cross section formulae for the production of heavy quarks with hard gluon bremsstrahlung are not available in the literature. In this paper we present compact analytic formulae for the cross-sections for the processes $Q+\bar{Q} \to g+g+\gamma$ and $Q+\bar{Q} \to q+\bar{q}+\gamma$. The cross-sections for the processes $\gamma+g \to Q+\bar{Q}+g$ and $\gamma+q \to Q+\bar{Q}+q$ can be obtained simply by crossing. With the help of these formulae we have estimated the contribution of these $2 \to 3$ processes at HERA energies using the Weizsäcker-Williams approximation for the electron-photon vertex. This is a good approximation since the production rate is dominated by the region of low electron transverse momenta. Therefore in high energy electron-proton scattering, the dominant parton-parton luminosity is provided by photon-gluon initial states, and the photons can be taken to be on their mass-shell. In

Fig. 1 we plot the parton luminosities calculated with the help of the formula,

$$\frac{d\mathcal{L}}{dM} = \frac{2M}{s}\int_\tau^1 \frac{dx}{x} F_{a/A}(x,M^2)F_{b/B}(\frac{\tau}{x},M^2), \tag{1.1}$$

where the function $F_{a/A}(x,M^2)$ denotes the number density of parton a in particle A. M and $\sqrt{s}$ are the parton and hadron centre of mass collision energies respectively and $\tau = M^2/s$. In the Weizsäcker-Williams approximation the number density of photons in the electron is,

$$F_{\gamma/e}(x) = \frac{\alpha}{2\pi} ln(\frac{\hat{s}}{4m_e^2})\left[\frac{1+(1-x)^2}{x}\right] \tag{1.2}$$

where m_e is the electron mass and x is the light-like fraction of the electron's momentum carried by the photon.

In the numerical evaluation of the gluon and quark wave functions, we used the EHLQ parametrisation[11], set 1. For the case of charm, (and perhaps for bottom), the quark mass is not large and the hadronic component of the electron given by the perturbative emission of an almost real photon and its subsequent decay into quarks and gluons can give non negligible contributions. In this case the gluon-gluon fusion and quark-antiquark annihilation mechanisms of heavy flavour production can also contribute. The Q^2 evolution of the gluon and quark number densities within the electron have been parametrised in Ref. [12]. We used their parametrisation with five flavours to calculate the gluon-gluon, gluon-quark and quark-antiquark luminosities of Fig. 2. Note that in the case of gg and $q\bar{q}$ initial states the short distance cross-sections are larger by the ratio of the coupling constants $O(\alpha_s/\alpha)$ than the cross-sections in the case of γg initial states. We can see from the comparison of the curves of Figs. 1 and 2 that at $\sqrt{s} = 314$ GeV the hadronic contribution of the electron becomes rapidly negligible above parton collision subenergies $\sqrt{\hat{s}} \approx 15$ GeV. This conclusion remains valid even after the inclusion of the exact hard scattering cross sections.

From this qualitative discussion we conclude that above parton subenergies of $O(\approx 15$ GeV) the dominant corrections to bottom production at HERA are the next to the leading order perturbative QCD corrections. We therefore study the hard gluon bremsstrahlung effects in some detail. In section III it is shown that the hard bremsstrahlung corrections to heavy quark pair production are less important in ep

collisions than in hadron-hadron collisions. This is to be expected since the simple argument which suggests that the gluon splitting mechanism will be large[13], makes no such prediction for the *ep* case. A complete theoretical analysis must include the full next to the leading order perturbative QCD corrections.

II. Cross Section Formulae

In electron-proton scattering heavy quark pairs can be produced at order $\alpha_s^2\alpha^2$ via the QCD subprocesses,

$$\gamma + g \quad \to Q + \bar{Q} \tag{2.1}$$

$$\gamma + q \quad \to Q + \bar{Q} + q \tag{2.2}$$

$$\gamma + g \quad \to Q + \bar{Q} + g \tag{2.3}$$

$$q + \bar{q} \quad \to Q + \bar{Q} \tag{2.4}$$

$$g + g \quad \to Q + \bar{Q}. \tag{2.5}$$

The physical cross sections are obtained by folding the subprocess cross sections with the photon wave function of the electron (which is of order α, see Eq. (1.2)) and the gluon or quark wave functions of the proton. In the case of the first subprocess (2.1) the one loop QCD corrections should also be taken into account. Our calculations and discussions will not be complete since we do not include these loop corrections.

The matrix element squared of the first subprocess is,

$$\gamma(p_1) + q(p_2) \to Q(p_3) + \bar{Q}(p_4)$$

$$\overline{\sum}\left|M_{\gamma g\to Q\bar{Q}}(p_1,p_2,p_3,p_4)\right|^2 = \frac{Vg^2e_H^2}{Np_{13}p_{23}}\left[p_{13}^2+p_{23}^2+2m^2p_{12}-\frac{m^4p_{12}^2}{p_{13}p_{23}}\right]. \tag{2.6}$$

where $V = N^2 - 1$ and N denotes the number of colours. Initial (final) colours and spins have been averaged (summed). m and e_H are the mass and charge of the heavy quark respectively. We denote the scalar product of two four momenta by,

$$p_{ij} = p_i \cdot p_j. \tag{2.7}$$

The spin and colour summed matrix elements squared for the subprocesses in Eqs. (2.2) and (2.3) are given in Tables 1 and 2, respectively. Averaging over initial colours and spins is not included. Note from Table 1 that the interference term A_3 predicts differing cross-sections for the production of a heavy quark and heavy antiquark.

It is interesting to note that the information given in Table 2, can be extracted from the expressions for the matrix element squared of the purely hadronic subprocess $Q\bar{Q}ggg$ calculated earlier[14,15]. This is most evident using the notation of ref.[14], where the matrix element squared for the subprocess $Q\bar{Q}ggg$ is expressed in terms of three independent colour structure functions which are proportional to N^4, N^2 and N^2+1, denoted by R_0, R_K and R_{QED} respectively. The colour structure function proportional to N^4 (R_0) is present only in the three gluon calculation. The other two functions are related to the functions which appear in the two gluon-one photon calculation presented in this paper. The function R_{QED} is proportional to the matrix element squared for the QED subprocess $Q\bar{Q}\gamma\gamma\gamma$. The colour structure function R_{KF} in Table 2 is related to the structure function R_K presented in ref.[14]. If we fully symmetrise R_{KF} in the gluon-gluon-photon labels (3,4,5) we obtain the colour structure function R_K of the $Q\bar{Q}ggg$ subprocess. These relations can be proven with some algebra directly from the colour and space-time symmetry properties of the Feynman diagrams describing the three subprocess $Q\bar{Q}\gamma\gamma\gamma$, $Q\bar{Q}gg\gamma$ and $Q\bar{Q}ggg$. They therefore provide a check of the correctness of our calculation.

For completeness we also give the matrix elements squared[16] for the subprocesses in Eqs. (2.4) and (2.5), summed (averaged) over final (initial) colours and spins,

$$q(p_1)+\bar{q}(p_2)\to Q(p_3)+\bar{Q}(p_4)$$

$$\overline{\sum}\left|M_{q\bar{q}\to Q\bar{Q}}(p_1,p_2,p_3,p_4)\right|^2=\frac{g^4V}{2N^2}\Big(\frac{p_{13}^2+p_{23}^2}{p_{12}^2}+\frac{m^2}{p_{12}}\Big) \tag{2.8}$$

and

$$g(p_1)+g(p_2)\to Q(p_3)+\bar{Q}(p_4)$$

$$\overline{\sum}\left|M_{gg\to Q\bar{Q}}(p_1,p_2,p_3,p_4)\right|^2=\frac{g^4}{2VN}\Big(\frac{V}{p_{13}p_{23}}-\frac{2N^2}{p_{12}^2}\Big)\left[p_{13}^2+p_{23}^2+2m^2p_{12}-\frac{m^4p_{12}^2}{p_{13}p_{23}}\right]. \tag{2.9}$$

We have studied the contributions of the subprocesses Eqs. (2.4) and (2.5) in order to determine the energy scale above which the these contributions become negligible. This is an important question from the point of view of quantitative description of heavy flavour production at HERA. When these contributions cannot be neglected, the next to the leading order analysis involves many terms and becomes quite cumbersome.

III. Numerical Results

We have calculated the contributions of all five subprocesses to heavy quark pair production cross sections in electroproduction using the Weizsäcker - Williams approximation at the electron photon vertex. We focused mainly on bottom production at HERA. Since the $2 \to 3$ processes are singular in configurations in which light partons are collinear, we require that the transverse momenta of the heavy quark pair in the final state is larger than the greater of 5 GeV and m. As a scale Q^2 in the structure functions and in the running coupling we used the value $Q^2 = (m^2 + p_\perp^2)$, where $p_\perp$ denotes the transverse momenta of the heavy quark. We assumed five flavours. All curves use the EHLQ, set 1 parametrisation of the gluon and quark wave function of the proton and the parametrisation of Ref. [12] for the quark and gluon wave functions of the electron.

In Fig. 3 we plotted total cross section for heavy flavour production at HERA energy ($\sqrt{s} = 314$ GeV) as a function of the heavy quark mass m. We can see that at low quark mass values the hadronic component of the electron can give important contributions. However, above the bottom production threshold these contributions become less important. The gluon-gluon fusion drops rapidly, while $q\bar{q}$ fusion and γq scattering with hard gluon bremsstrahlung give $\approx 15\%$ corrections. It is also evident from the curve that the subprocess of Eq. (2.2) gives the most important corrections at very high quark mass values. We note that in a similar treatment in hadron-hadron collisions, with a cut of 5 GeV on the $p_\perp$ of the final gluon, bremsstrahlung corrections are found to be much larger[7,9].

In Fig. 4 we plot the energy dependence of bottom pair production. It can be seen that above HERA energies the most important corrections are given by gluon-gluon fusion. This is not unexpected since at high energies the bottom quarks

are produced at small x values. Note, however that the gluon component of the electron is not known and that parametrisation of Ref. [12] is only an educated guess. In Fig. 5 we have plotted the rapidity distributions for bottom production at HERA energies (E_e = 30 GeV and E_p = 830 GeV). The curves of this figure reflect the obvious kinematical consequences of the asymmetric beam energies and the x-behaviour of the structure functions. In Fig. 6 the transverse momentum distribution of the bottom quark is given. For the high $p_\perp$ tail the bremsstrahlung corrections are more important. This behaviour is similar to the case of hadron hadron collisions but less pronounced. Finally in Fig. 7 we plotted the $p_\perp$ distribution of the $b\bar{b}$ system. This is the only quantity which is completely given by the $2 \to 3$ subprocess of Eqs. (2.2) and (2.3). We see that at large $p_\perp$ values the Bethe-Heitler type subprocess Eq. (2.2) can compete with the photon-gluon fusion contribution, Eq. (2.3). The shape of the curve at smaller values of $p_\perp$ is expected to be modified by Sudakov-type higher order double logarithmic corrections in analogy with the modification to the shape of the $p_\perp$ distribution of the W-boson produced in $p\bar{p}$ collisions[17].

IV. Discussion and Conclusions

We have presented compact expressions for the cross sections of the $2 \to 3$ subprocesses Eqs. (2.2,2.3). Using these expressions we have estimated the importance of hard gluon bremsstrahlung effects for heavy quark pair production at HERA. In contrast to case of hadron collisions we do not find any anomalously large effect. This is in accord with our expectation, since in the case of photoproduction the gluon splitting mechanism is not favoured by a large cross-section for the production of gluon jets. We have also considered the contributions given by the hadronic component of the electron. Here there is potentially a problem of double counting. The splitting of the photon into collinear quark pair is partially included in the contribution of the subprocess of Eq. (2.2). This subprocess mainly contributes in the kinematical region of low $b\bar{b}$ transverse momenta. Therefore, qualitatively, we have separated the two contributions. More work is needed for the clean separation of the low $p_\perp$ and large $p_\perp$ regimes.

We find that at higher parton subprocess energies the contributions given by the hadronic component of the electron become negligible. Therefore, at HERA, at

parton subenergies greater than $\approx$ 15 GeV, bottom and charm production can be described quantitatively in terms of the leading contribution (2.1) and its next to the leading order perturbative QCD corrections. Such an analysis of future measurements at HERA will be complementary to the study of heavy flavour production in hadron-hadron collisions. The experimental study of bottom and charm production in this kinematical region will help to measure the gluon wave function more precisely and will also improve our understanding of the QCD description of heavy quark production in hadron-hadron, photon-hadron and electron-hadron collisions.

ACKNOWLEDGEMENT. One of us (Z.K.) acknowledges the cordial hospitality of the theory group at Fermilab where this work was performed.

REFERENCES

[1] For a review on charm production see A. Kernan and G. VanDalen, *Phys. Rep.* **106** (1984) 298 .

[2] J. P. Albanese *et al.*, *Phys. Lett.* **158B** (1983) 51 ;
M. G. Catanesi *et al.*, *Phys. Lett.* **187B** (1987) 431 .

[3] C. Albjar *et al.*, *Phys. Lett.* **186B** (1987) 237 .

[4] C. Albjar *et al.*, CERN-EP/87-190 (1987).

[5] B. Wiik, *Acta. Phys. Pol.* **B16** (1985) 127 .

[6] J. C. Collins, D. E. Soper and G. Sterman, *Nucl. Phys.* **B263** (1986) 37 .

[7] Z. Kunszt, E. Pietarinen and E. Reya, *Phys. Rev.* **D21** (1980) 733 .

[8] L. Schmitt, L. M. Seghal, H. D. Toll and P. M. Zerwas,
Phys. Lett. **139B** (1984) 99 ;
E. W. N. Glover, K. Hagiwara and A. D. Martin, *Phys. Lett.* **139B** (1986) 99 .

[9] B. van Eijk, PhD Thesis, Amsterdam (1986);
A. Ali, B. van Eijk and I. ten Haven, *Nucl. Phys.* **B292** (1987) 1 .

[10] P. Nason, S. Dawson and R. K. Ellis, Fermilab-Pub-87/222-T, (December 1987).

[11] E. Eichten, I. Hinchliffe, K. Lane, and C. Quigg, *Rev. Mod. Phys.* **56** (1984) 247 , Errata, *Rev. Mod. Phys.* **58** (1986) 1065 .

[12] M. Drees and K. Grassie, *Zeit. Phys.* **C28** (1985) 451

[13] Z. Kunszt and E. Pietarinen, *Nucl. Phys.* **164B** (1980) 45 .

[14] J. F. Gunion and Z. Kunszt, *Phys. Lett.* **178B** (1986) 296 .

[15] R. K. Ellis, in Proceedings of the XXI Rencontre de Moriond: Strong interactions and gauge theories, Les Arcs, France (1986);
R. K. Ellis and J. C. Sexton, *Nucl. Phys.* **B282** (1987) 642 .

[16] B. L. Combridge, *Nucl. Phys.* **B151** (1979) 429 ;
L. M. Jones and H.W. Wyld, *Phys. Rev.* **D17** (1978) 1782 ;
M. Glück, J. F. Owens and E. Reya, *Phys. Rev.* **D17** (1979) 760 .

[17] G. Parisi and R. Petronzio, *Nucl. Phys.* **B154** (1979) 427 ;
J. C. Collins and D. E. Soper, *Nucl. Phys.* **B197** (1982) 446 ;
G. Altarelli, R. K. Ellis and G. Martinelli, *Nucl. Phys.* **B242** (1984) 120 .

FIGURE CAPTIONS

Figure 1: Luminosity functions for initial parton combinations γg and γq (see Eq.(1.1) in ep collisions at energy $\sqrt{s} = 314\ GeV$. M denotes the subenergy of the parton collisions.

Figure 2: Luminosity function of gg, gq, $\bar{q}q$ and $q\bar{q}$ parton collisions in electron proton scattering at HERA energies.

Figure 3: Total cross section for heavy quark production in ep collisions as a function of the heavy quark mass at HERA ($\sqrt{s} = 314\ GeV$). The

contributions of the five production mechanisms (2.1) - (2.5) are separately indicated. The charge of the heavy quark is taken to be $-\frac{1}{3}$.

Figure 4: Total cross section for bottom quark production in ep collisions as a function of the collision energy. The contributions of the five production mechanisms (2.1) - (2.5) are separately indicated.

Figure 5: Rapidity distributions for bottom pair production in ep collisions at HERA energy. The contributions of the five production mechanisms (2.1) - (2.5) are separately indicated.

Figure 6: Transverse momentum distribution of the bottom quark produced in ep collisions at HERA energy. The contributions of the five production mechanisms (2.1) - (2.5) are separately indicated.

Figure 7: Transverse momentum distribution of the pair of bottom quarks produced in ep collisions at HERA energy. The contributions of the five production mechanisms (2.1) - (2.5) are separately indicated.

TABLE CAPTIONS

Table 1: Spin and color summed matrix element squared for the subprocess:

$$Q(-p_1) + \bar{Q}(-p_2) \to q(p_3) + \bar{q}(p_4) + \gamma(p_5).$$

The heavy quark mass is m, $(p_1^2 = p_2^2 = m^2, p_i^2 = 0, i = 3,4,5)$ and the invariants are defined as $p_{ij} = p_i \cdot p_j$ and $s = (p_1 + p_2)^2$. The electric charge of the massive and massless quarks rare denoted by e_H and e_L respectively.

Table 2: Spin and color summed matrix element squared for the subprocess,

$$Q(-p_1) + \bar{Q}(-p_2) \to g(p_3) + g(p_4) + \gamma(p_5).$$

m denotes the heavy quark mass $(p_1{}^2 = p_2{}^2 = m^2, p_i{}^2 = 0, i = 3,4,5)$ and the invariants are defined as $p_{ij} = p_i \cdot p_j$ and $s = (p_1 + p_2)^2$. The R_{QED} part has to be summed over 12 permutations corresponding to

the 6 permutations of the momenta p_3, p_4, p_5 and two permutations of the momenta p_1 and p_2. R_{KF} has to be summed over 4 permutations corresponding to the interchange of p_1, p_2 and p_3, p_4.

$$A_1 = \frac{(p_{13}^2+p_{23}^2+p_{14}^2+p_{24}^2+m^2s)p_{12}}{p_{15}p_{25}sp_{34}} + \frac{m^2(p_{35}^2+p_{45}^2)}{2p_{34}^2p_{15}p_{25}}$$
$$+\frac{m^2(p_{13}^2+p_{14}^2+p_{23}^2+p_{24}^2-sp_{34})}{sp_{34}^2}\left[\frac{1}{p_{15}}+\frac{1}{p_{25}}\right]$$
$$-\frac{m^2}{2p_{34}^2}\left[\frac{p_{13}^2+p_{14}^2+m^2p_{34}}{p_{25}^2}+\frac{p_{23}^2+p_{24}^2+m^2p_{34}}{p_{15}^2}\right]$$

$$A_2 = \frac{p_{13}^2+p_{23}^2+p_{14}^2+p_{24}^2+2m^2p_{34}}{sp_{35}p_{45}} + \frac{2m^2(p_{35}^2+p_{45}^2)}{s^2p_{35}p_{45}}$$

$$A_3 = \frac{p_{13}^2+p_{23}^2+p_{14}^2+p_{24}^2+m^2(p_{34}+\frac{1}{2}s)}{sp_{34}}\left[\frac{p_{13}}{p_{15}p_{35}}+\frac{p_{24}}{p_{25}p_{45}}-\frac{p_{14}}{p_{15}p_{45}}-\frac{p_{23}}{p_{25}p_{35}}\right]$$
$$+\frac{2m^2}{sp_{34}}\left[\frac{(p_{23}-p_{24})}{p_{15}}+\frac{(p_{14}-p_{13})}{p_{25}}\right]$$

$$\sum \mid M_q \mid^2 = 4Vg^4(c_H^2A_1+c_L^2A_2+c_Hc_LA_3)$$

Table 1

$$R_{QED} = \frac{sp_{13}^2}{8p_{14}p_{24}p_{15}p_{25}}$$

$$-\frac{m^2}{2p_{25}}\left[\frac{1}{p_{14}}\left(\frac{s}{2p_{24}}+\frac{p_{23}}{p_{14}}-3\right)+\frac{(p_{15}+p_{23}-p_{14})}{2p_{13}p_{24}}-\frac{1}{p_{15}}+\frac{3}{2p_{24}}\right]$$

$$-\frac{m^4}{2p_{25}p_{14}}\left[\frac{1}{2p_{24}}\left(\frac{p_{24}-3p_{14}-2p_{15}}{p_{13}}-\frac{3p_{13}}{p_{15}}-4\right)-\frac{2}{p_{25}}\right]$$

$$+\frac{m^6}{p_{25}p_{14}}\left[\frac{1}{2p_{24}}\left(\frac{1}{2p_{15}}+\frac{1}{p_{13}}\right)+\frac{1}{2p_{14}}\left(\frac{1}{2p_{25}}+\frac{1}{p_{23}}\right)\right]$$

$$R_{KF} = -\frac{1}{2p_{34}}\left[\frac{p_{15}^2}{p_{24}p_{13}}+\frac{p_{14}^2}{p_{15}p_{25}}\left(\frac{p_{14}}{p_{13}}+\frac{p_{24}}{p_{23}}\right)\right]$$

$$+\frac{m^2}{2p_{34}^2}\left[1-\frac{2p_{14}}{p_{25}}\left(\frac{p_{14}}{p_{25}}+\frac{p_{23}}{p_{15}}\right)\right]+\frac{m^2}{4p_{14}p_{23}}\left[\frac{2p_{15}}{p_{23}}+\frac{2(p_{15}+p_{25})}{p_{34}}-7\right]$$

$$+\frac{m^2}{2p_{25}p_{14}}\left[\frac{p_{15}-p_{34}}{p_{23}}+\frac{p_{34}+p_{23}}{p_{15}}+\frac{p_{23}}{p_{14}}-\frac{p_{34}}{p_{25}}-7\right]$$

$$+\frac{m^2}{p_{25}}\left[\frac{1}{p_{34}}\left(\frac{p_{15}+p_{14}}{p_{23}}-\frac{2p_{14}}{p_{25}}-\frac{2p_{14}}{p_{15}}-2\right)-\frac{1}{p_{15}}-\frac{3}{2p_{25}}\right]$$

$$+\frac{m^4}{p_{25}p_{23}}\left[\frac{1}{p_{34}}\left(\frac{p_{15}}{p_{14}}+\frac{p_{14}}{p_{15}}\right)+\left(\frac{p_{34}}{p_{14}}-2\right)\frac{1}{2p_{15}}\right]$$

$$+\frac{m^4}{p_{25}}\left[\frac{1}{p_{34}}\left(\frac{1}{p_{23}}-\frac{1}{p_{25}}-\frac{1}{p_{14}}-\frac{2}{p_{15}}\right)-\frac{1}{p_{14}}\left(\frac{1}{p_{14}}+\frac{1}{p_{25}}+\frac{2}{p_{23}}\right)\right]$$

$$+\frac{m^4}{p_{14}p_{23}}\left(\frac{1}{2p_{34}}-\frac{1}{p_{14}}\right)-\frac{m^6}{p_{14}^2}\left[\left(\frac{1}{2p_{25}}+\frac{p_{14}}{2p_{23}p_{15}}\right)^2+\left(\frac{1}{4p_{23}}+\frac{1}{p_{25}}\right)\frac{1}{p_{23}}\right]$$

$$\sum |\, M_g \,|^2 = -4g^4e_H^2V/N\left[(R_{QED}+11 \text{ perm's.})+N^2(R_{KF}+3 \text{ perm's.})\right]$$

Table 2

Figure 1

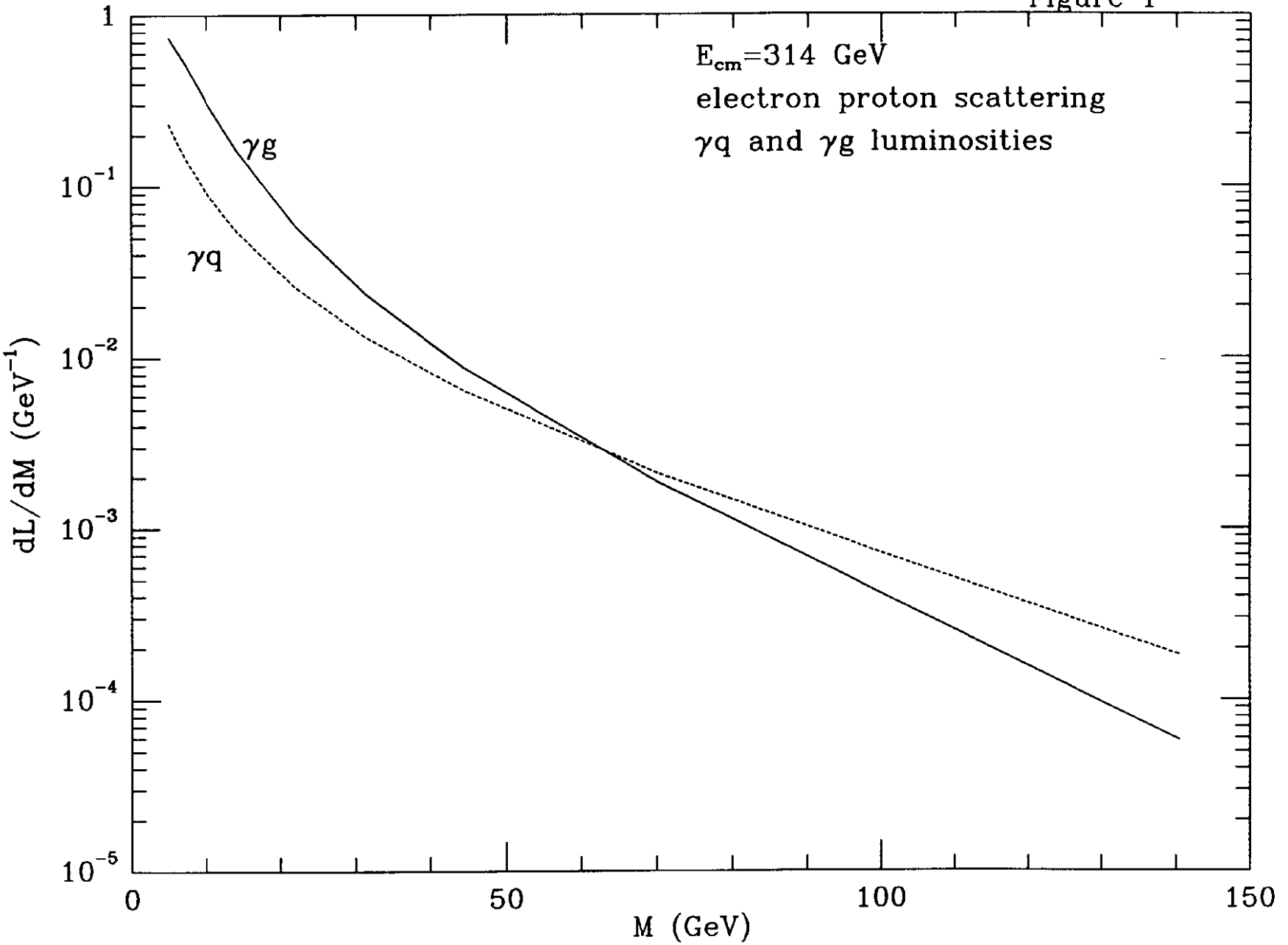
E_{cm}=314 GeV
electron proton scattering
γq and γg luminosities
γg
γq
dL/dM (GeV^{-1})
M (GeV)
1
10^{-1}
10^{-2}
10^{-3}
10^{-4}
10^{-5}
0
50
100
150

Figure 2

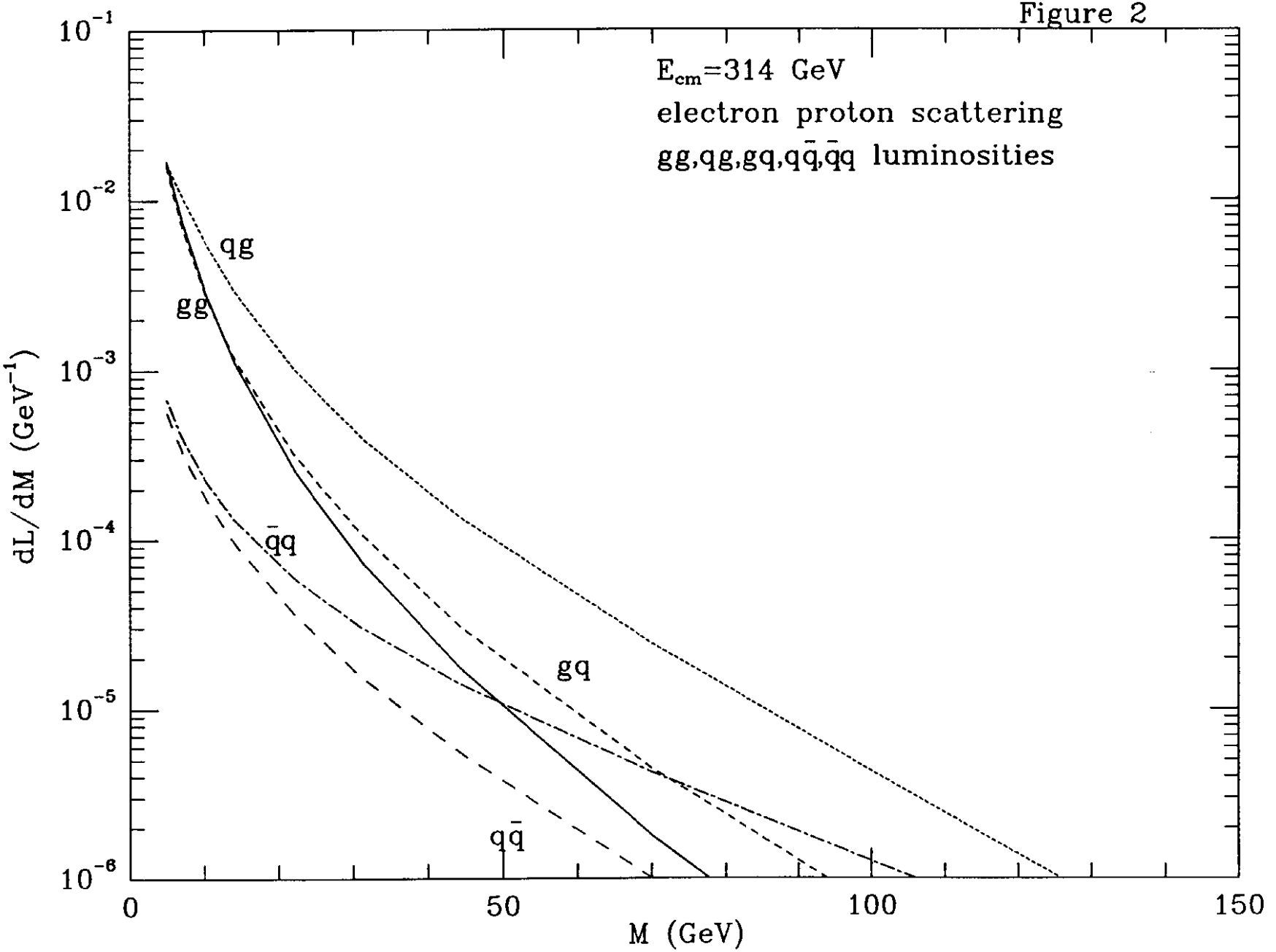
E_{cm}=314 GeV
electron proton scattering
gg,qg,gq,q$\bar{q}$,$\bar{q}$q luminosities
qg
gg
$\bar{q}$q
gq
q$\bar{q}$
10^{-1}
10^{-2}
10^{-3}
10^{-4}
10^{-5}
10^{-6}
dL/dM (GeV^{-1})
0
50
100
150
M (GeV)

Figure 3

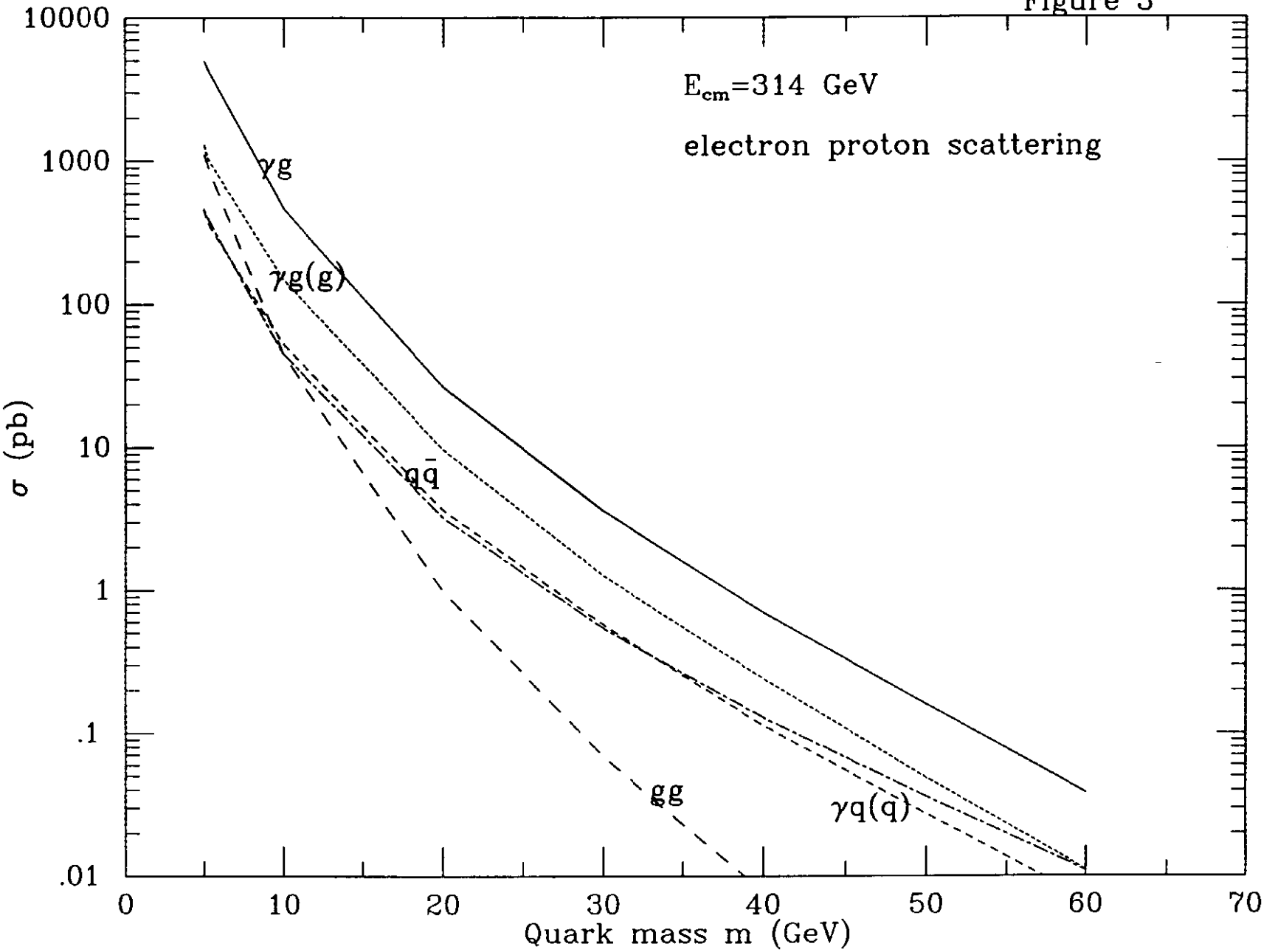
10000
1000
100
10
1
.1
.01
σ (pb)
0
10
20
30
40
50
60
70
Quark mass m (GeV)
E_{cm}=314 GeV
electron proton scattering
γg
γg(g)
qq̄
gg
γq(q̄)

Figure 4

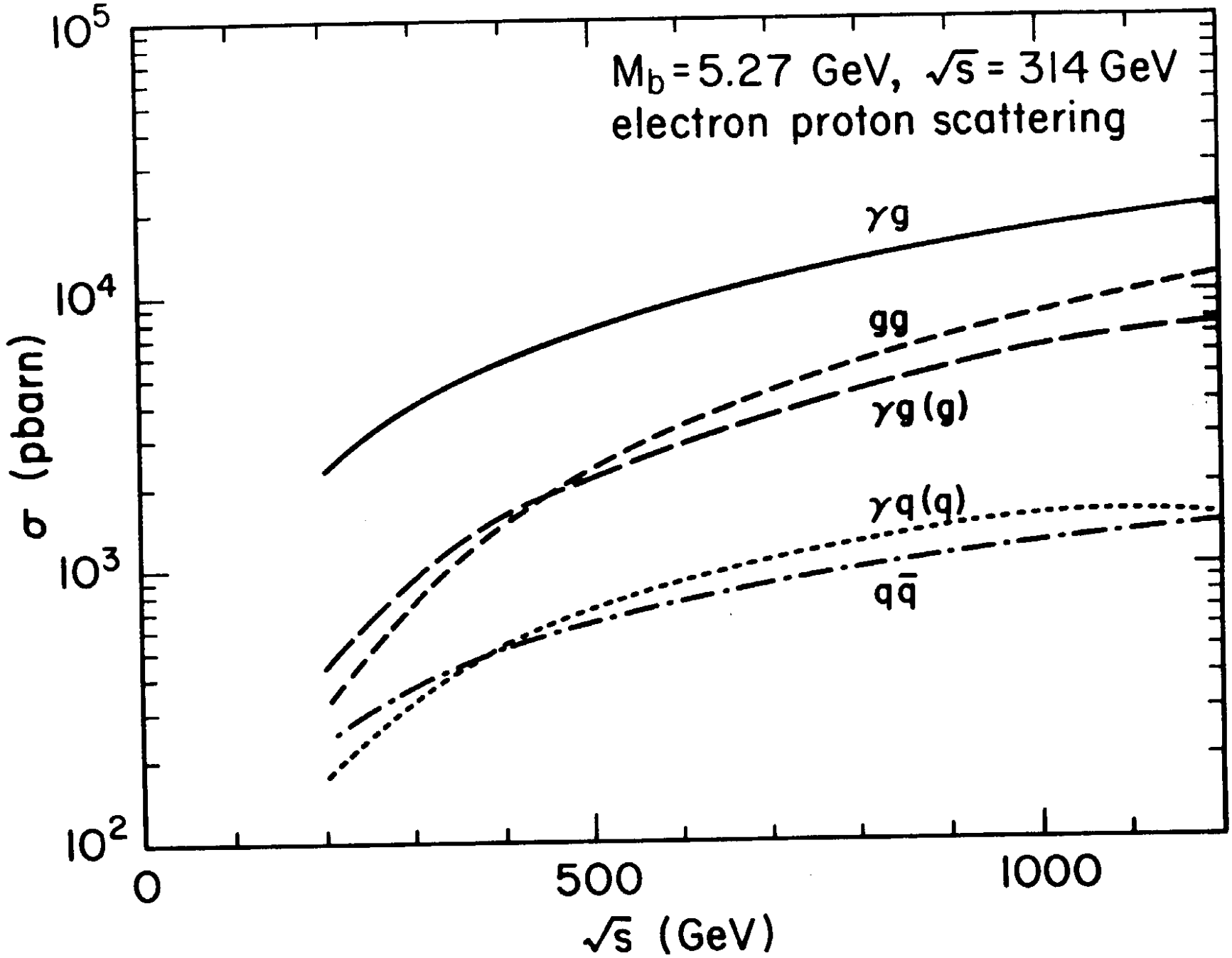
$M_b = 5.27$ GeV, $\sqrt{s} = 314$ GeV
electron proton scattering
γg
gg
$\gamma g\,(g)$
$\gamma q\,(q)$
$q\bar{q}$
10^5
10^4
10^3
10^2
σ (pbarn)
0
500
1000
$\sqrt{s}$ (GeV)

Figure 5

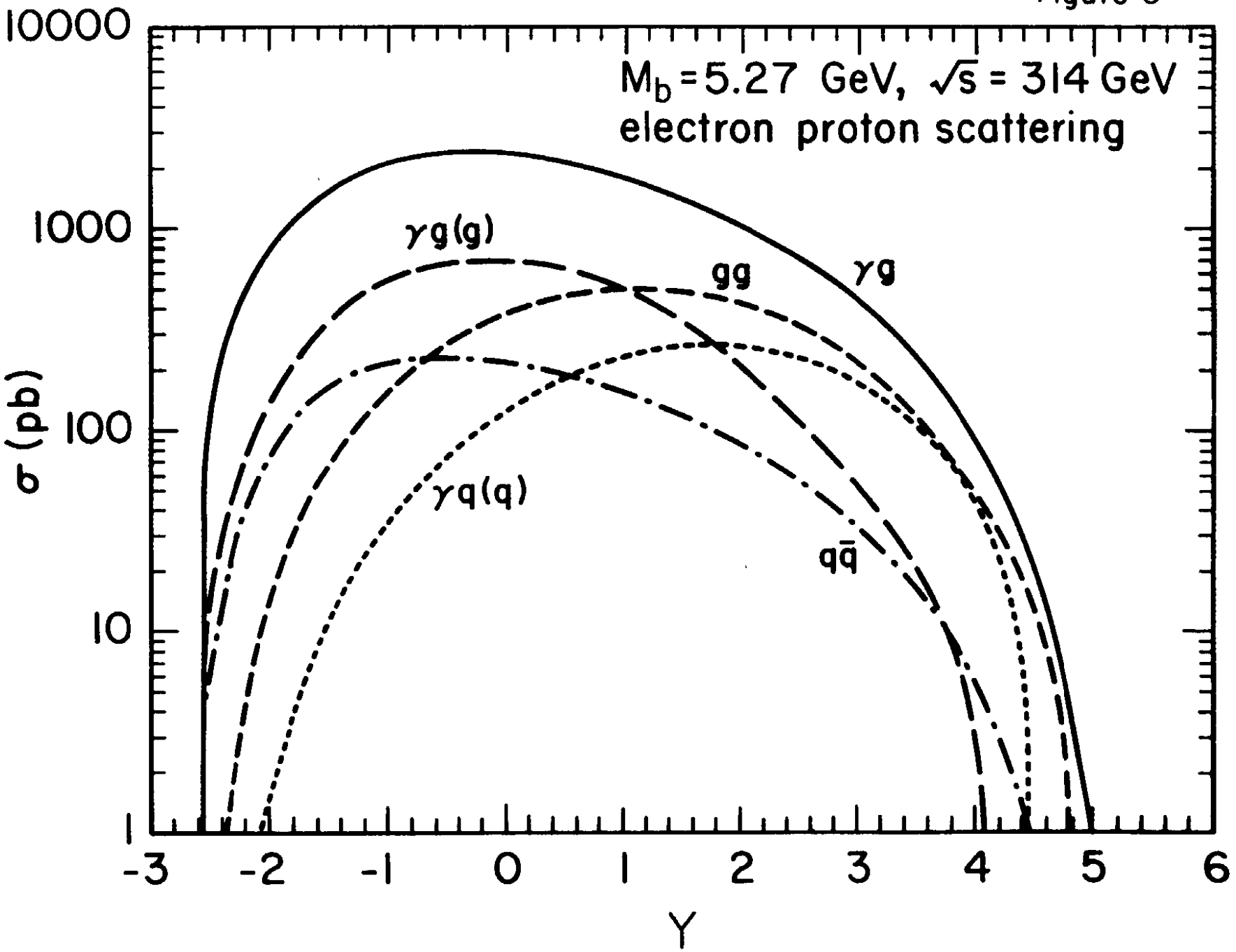
M_b = 5.27 GeV, $\sqrt{s}$ = 314 GeV
electron proton scattering
γg(g)
gg
γg
γq(q)
qq̄
σ (pb)
10000
1000
100
10
1
-3
-2
-1
0
1
2
3
4
5
6
Y

Figure 6

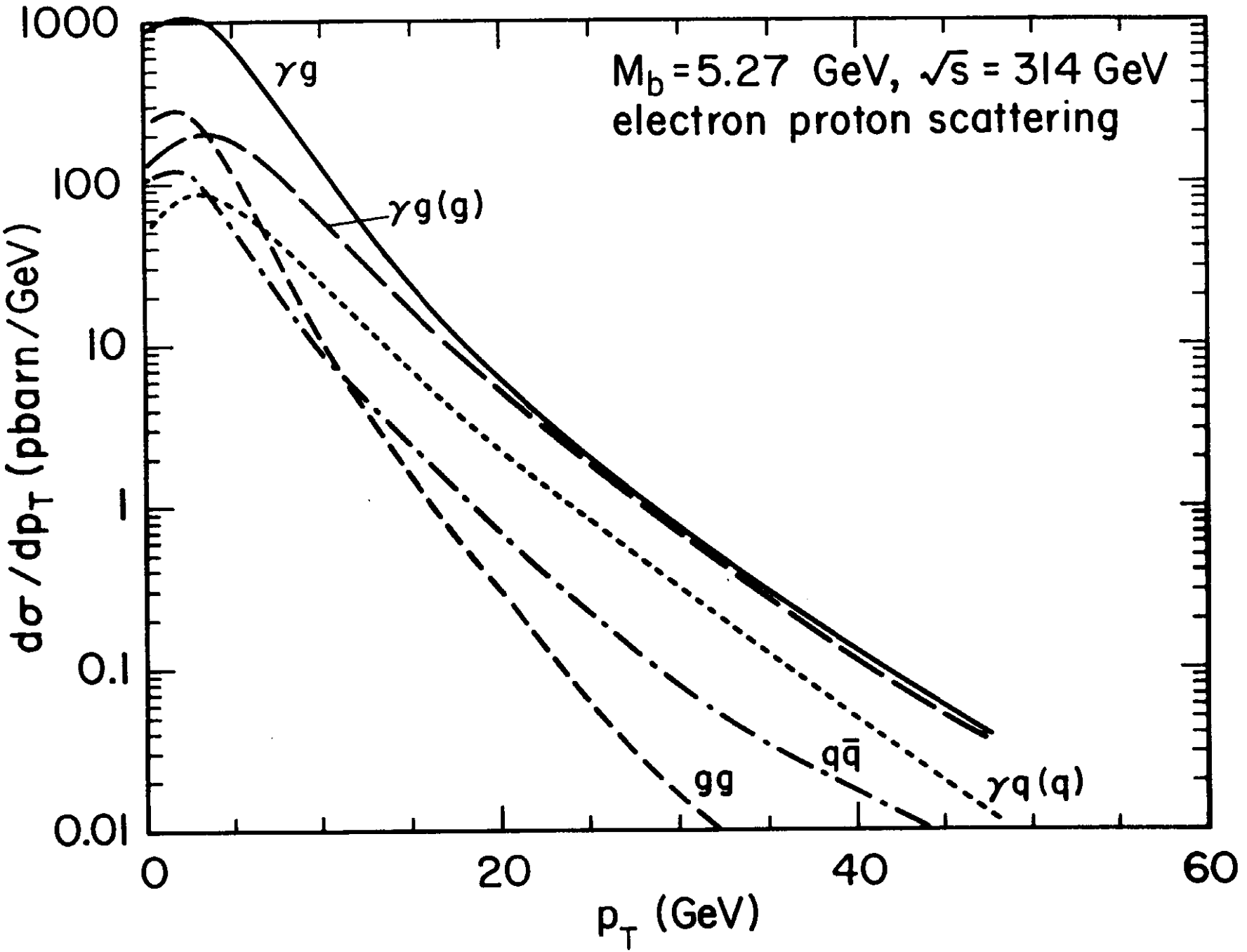
1000
100
10
1
0.1
0.01
0
20
40
60
$d\sigma/dp_T$ (pbarn/GeV)
p_T (GeV)
$M_b = 5.27$ GeV, $\sqrt{s} = 314$ GeV
electron proton scattering
γg
$\gamma g(g)$
$q\bar{q}$
gg
$\gamma q(q)$

Figure 7

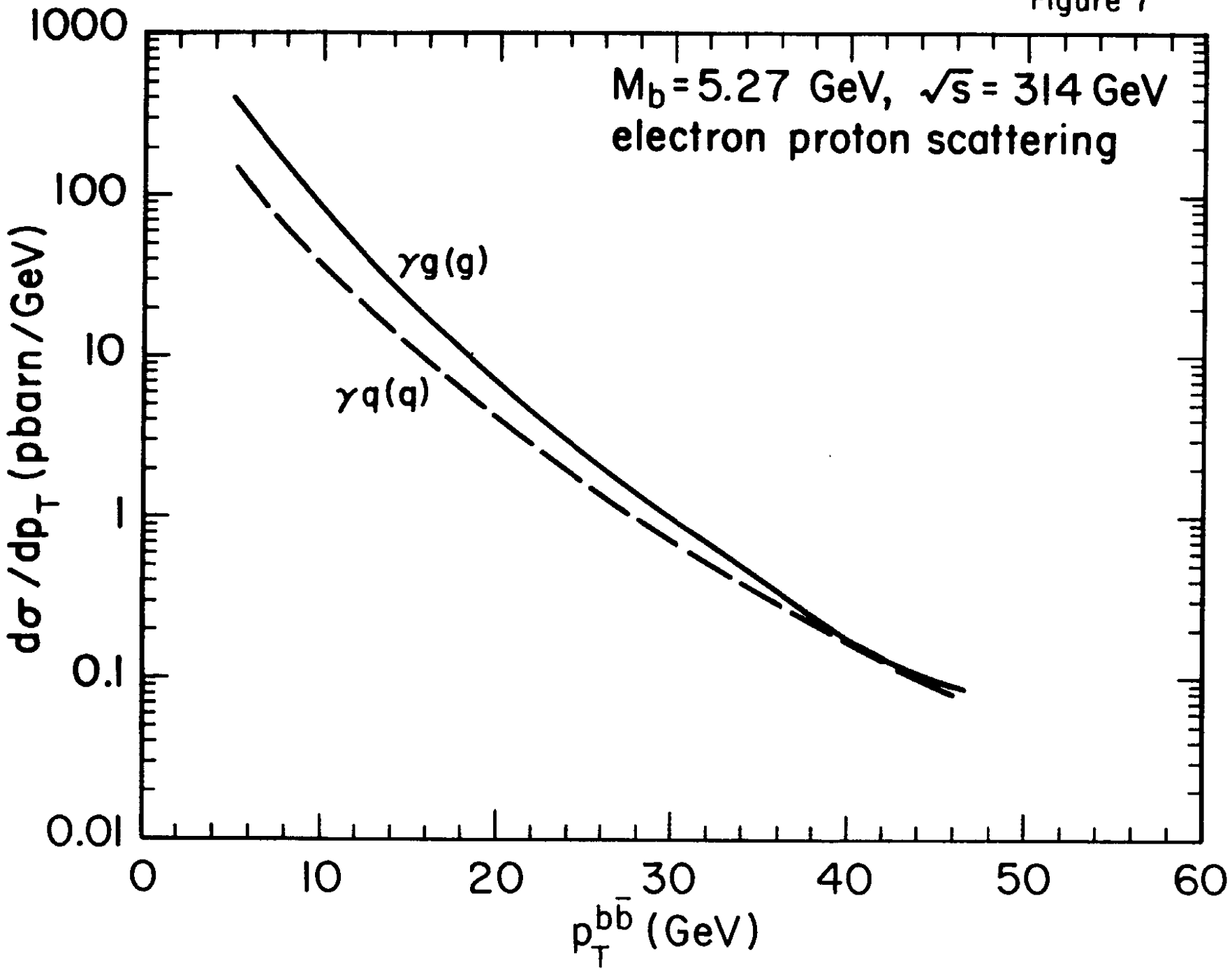
1000
100
10
1
0.1
0.01
$d\sigma/dp_T$ (pbarn/GeV)
$M_b = 5.27$ GeV, $\sqrt{s} = 314$ GeV
electron proton scattering
$\gamma g(g)$
$\gamma q(q)$
0
10
20
30
40
50
60
$p_T^{b\bar{b}}$ (GeV)